
PQPP: A Joint Benchmark for Text-to-Image Prompt and Query Performance Prediction

Eduard Poesina[◇]
University of Bucharest

Adriana Valentina Costache[◇]
University of Bucharest

Adrian-Gabriel Chifu
Aix-Marseille Université

Josiane Mothe
Université Toulouse Jean-Jaurès

Radu Tudor Ionescu^{*}
University of Bucharest

Abstract

Text-to-image generation has recently emerged as a viable alternative to text-to-image retrieval, due to the visually impressive results of generative diffusion models. Although query performance prediction is an active research topic in information retrieval, to the best of our knowledge, there is no prior study that analyzes the difficulty of queries (prompts) in text-to-image generation, based on human judgments. To this end, we introduce the first dataset of prompts which are manually annotated in terms of image generation performance. In order to determine the difficulty of the same prompts in image retrieval, we also collect manual annotations that represent retrieval performance. We thus propose the first benchmark for joint text-to-image prompt and query performance prediction, comprising 10K queries. Our benchmark enables: (i) the comparative assessment of the difficulty of prompts/queries in image generation and image retrieval, and (ii) the evaluation of prompt/query performance predictors addressing both generation and retrieval. We present results with several pre-generation/retrieval and post-generation/retrieval performance predictors, thus providing competitive baselines for future research. Our benchmark and code is publicly available under the CC BY 4.0 license at <https://github.com/Eduard6421/PQPP>.

1 Introduction

In recent years, more and more people embraced the use of large language models (LLMs) instead of traditional search engines [1, 5, 53]. The advent of generative diffusion models [7, 15, 30, 36] capable of generating high-quality and realistic images triggered a similar trend in text-to-image retrieval. This paradigm shift in information retrieval (IR) calls for an extensive exploration of research topics related to generative models. For instance, query performance prediction (QPP) is an active research topic in IR [10, 13, 18, 27, 32]. QPP refers to the process of estimating the performance level of an IR system for a given query [6]. Assessing the difficulty of a query before retrieving the results can help an IR system take informed decisions about query optimization strategies, indexing, query-specific tuning, and so on. To the best of our knowledge, there is no prior study that analyzes the difficulty of queries (prompts) in text-to-image generation and retrieval using human relevance judgments.

In this study, we introduce the first dataset of prompts which are manually annotated in terms of image generation performance. We collected over 240K relevance judgments from 147 human annotators for 40K images generated by diffusion models in response to 10K prompts. We select these prompts from the Microsoft Common Objects in Context (MS COCO) dataset [26], which comprises images with captions. We chose MS COCO as a well-established data collection that allows cross-task

^{*}Corresponding author: raducu.ionescu@gmail.com. [◇]Equal contribution.

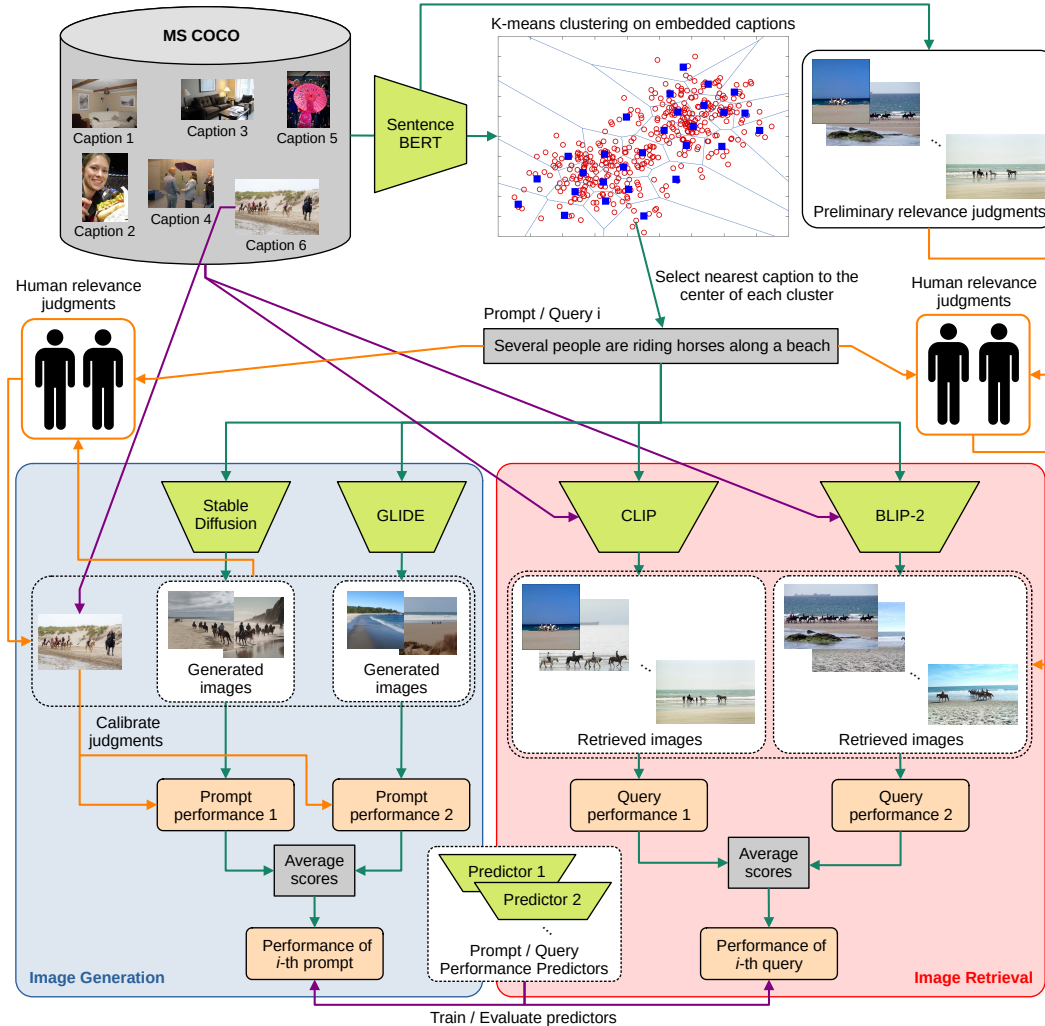


Figure 1: We select a set of 10K captions from MS COCO [26] using k-means clustering. Next, we collect human relevance judgments in two scenarios: image generation and image retrieval. For each prompt/query, we generate images with two diffusion models (Stable Diffusion [36] and GLIDE [30]) and retrieve images from MS COCO with two vision-language models (CLIP [33] and BLIP-2 [24]). Based on the collected relevance judgments, we score each prompt/query in terms of generation and retrieval performance, respectively. Finally, we train and evaluate multiple prompt/query performance predictors on the proposed benchmark. Best viewed in color.

studies and is cost-effective. It provides high-quality image annotations, as well as a wide range of everyday scenes and objects. To select a representative and diverse set of prompts from over 590K captions in MS COCO, we employ a k-means clustering algorithm on the embedding space of a sentence BERT model [42], where $k = 10,000$. We extract the closest caption to each cluster center to build our set of prompts. For each prompt, we generate two images with Stable Diffusion [36] and two with GLIDE [30]. Further, we aim to study the same set of 10K prompts from two perspectives: generation performance and retrieval performance. To this end, we collect another set of 1.25M annotations from 91 human evaluators to obtain ground-truth relevance judgments for the retrieval task. We start from preliminary relevance judgments determined via the pre-trained sentence BERT [42] applied on captions. If a caption from MS COCO is similar to a query in the BERT embedding space, the image corresponding to the respective caption is added to the set of images that are potentially relevant to the respective query. Next, we collect human relevance judgments for all 10K queries. The retrieval difficulty score of each query is estimated with respect to two state-of-the-art vision-language models, CLIP [33] and BLIP-2 [24], which are tasked with retrieving

images for all 10K queries. The entire process used to develop the Prompt and Query Performance Prediction (QPP) benchmark is illustrated in Figure 1.

We conduct preliminary experiments to compare prompt/query difficulty in image generation versus image retrieval. Our findings show that there is a very low correlation between the two tasks, which justifies the need to study the novel task of prompt performance prediction in image generation. We also carry out experiments with multiple pre- and post-generation/retrieval performance predictors, providing a set of competitive baselines for future research. We find that a strong supervised pre-generation/retrieval predictor is a worthy competitor for post-generation/retrieval predictors in both text-to-image generation and retrieval.

In summary, our contribution is threefold:

- We propose the first joint benchmark for prompt and query performance prediction.
- We collect nearly 1.5M relevance judgments from human annotators to score a total of 10K queries in terms of generation and retrieval performance.
- We experiment with multiple pre-generation/retrieval and post-generation/retrieval performance predictors to obtain competitive results, which serve as baselines for future work.

2 Related Work

Studies on QPP initially focused on textual ad hoc retrieval, where both pre- and post-retrieval predictors were considered for sparse retrieval models [8, 22, 29, 48]. Some recent studies investigated dense (neural network) retrieval models [2, 10, 11, 18, 49], as well as diverse tasks, such as conversational search [19, 27, 37]. We discuss QPP in textual ad hoc retrieval in Appendix A.4.

QPP in text-to-image retrieval/generation. QPP in a multimodal (e.g. text-to-image) context is a relatively new research area [4, 23, 31, 45, 46]. The exploration of QPP in the context of text-to-image retrieval and generation is gaining significant interest, particularly with the rapid advancements in generative methods [7]. This research domain, distinct for its multimodal nature, aims to enhance the prediction of text query effectiveness for retrieving relevant images. Initial studies, such as those of Xing et al. [47] and Tian et al. [43, 44], have laid the groundwork by exploring query difficulty prediction in image retrieval, utilizing machine learning algorithms and assessing the utility of various features and information sources.

Further contributions by Li et al. [25] delve into the challenges of estimating query difficulty with unigram language models and visual word verification, highlighting the complexities of aligning text-based queries with visual data. Meanwhile, the development of a self-supervised framework for Content-Based Image Retrieval (CBIR) systems marks a significant advancement [45], addressing the scarcity of labeled data through synthetic data and rank-based feature training. Recent efforts, such as those of Wu et al. [46] and Pavlichenko and Ustalov [31], focus on integrating human feedback into text-to-image models to refine prediction accuracy and enhance the visual appeal of generated images. Kumari et al. [23] introduced an approach to concept ablation in text-to-image synthesis, aiming to selectively prevent the generation of specific concepts.

The closest work to our research is that of Bizzozzero et al. [4], which introduced the concept of *prompt performance prediction*. The authors assessed the effectiveness of prompts in generating images. However, in their study, the ground-truth is automatically generated, which may introduce a significant bias in the evaluation. In contrast, we are the first to explore the prompt performance prediction task with respect to human relevance judgments. In addition, we introduce a benchmark that provides performance measurements for the same set of prompts/queries in both generation and retrieval, enabling the comparative study of QPP across both tasks. Another novel contribution of our work is the study of post-generation prompt performance predictors.

QPP evaluation. To evaluate QPP, one should determine the degree of dependence between the predicted performance and the actual performance obtained by an IR system. A correlation test serves this purpose and, for this reason, it is widely used. Some studies have highlighted the limitation of correlation coefficients for evaluating QPP in certain scenarios [17, 21, 28], and suggested alternative measures, such as the scaled Absolute Ranking Error (sARE) and its mean (sMARE) to model performance using distributions [17]. Although we agree that correlation may not be the only way to evaluate QPP, we choose to use it in the evaluation part of our study due to its wide adoption in QPP literature.



Figure 2: An example showing the annotation interface for a random prompt and the images associated with the respective prompt. For each image, the annotator can select one of the following options: high relevance, low relevance, no relevance and unrealistic. The relevance judgments of an annotator are shown for illustrative purposes. Best viewed in color.

3 Proposed Benchmark

To develop our novel Prompt and Query Performance Prediction (PQPP) benchmark, we harness the images and captions from the MS COCO [26] training set, which comprises approximately 118K images. Each of these images is accompanied by 5 to 7 descriptive captions, providing a rich context for our study.

To establish a unified foundation for text-to-image generation and retrieval, we select a subset of 10,000 captions to be used across tasks either as *queries* for text-to-image retrieval, or as *prompts* for text-to-image generation. We aim for a wide variety of captions that can be clearly associated with images. The selection process entails identifying the most relevant caption for each image (from the set of captions available in MS COCO for the respective image), where the (caption, image) similarity is measured via the cosine similarity in the CLIP embedding space [33]. This reduces the number of captions to about 118K. The resulting captions are further processed by a sentence transformer based on BERT [42] to extract sentence embeddings. Aiming to enhance the distinctiveness of our final set of captions, we next apply the k-means clustering algorithm based on k-means++ initialization on the extracted embeddings. For each cluster, we select the nearest caption to the center of each cluster and include it in our final set of captions. We set $k = 10,000$, thus obtaining a set of 10K prompts/queries. We next describe the procedures for collecting human relevance judgments for text-to-image generation and text-to-image retrieval in separate sections.

3.1 Prompt Performance Assessment

Generative models. To generate images for the established set of prompts, we employ the well-established Stable Diffusion [36] and GLIDE [30] generative models. For the first model, we choose the Stable Diffusion XL (base-1.0) variant, which produces images with a resolution of 1024×1024 pixels. In contrast, GLIDE initially produces images at a resolution of 64×64 pixels. The images are subsequently upsampled to a resolution of 256×256 pixels using the upsampling model integrated in GLIDE. For each prompt, we generate two images with Stable Diffusion and two images with GLIDE.

Control and calibration. Along with the four generated images, we include the image from MS COCO associated with each prompt into the annotation process. The ground-truth image is included to calibrate user annotations (assuming that the ground-truth image should be labeled as highly relevant) or to exclude annotators that are not seriously engaged in the annotation process. To further ensure the quality of human relevance judgments, we implement a verification process based on a control set of 100 prompts. The control prompts are independently annotated by three authors of this study, following the same protocol as the other annotators. The Fleiss’ κ coefficient among the control annotators is 0.55. While running the full-scale annotation process, a control prompt is randomly inserted among every five prompts. This allows us to set a minimum threshold for the Cohen’s κ coefficient to accept the relevance judgments of an annotator. The relevance judgments of an annotator are included into the study if the respective annotator (i) has at least a moderate agreement² ($\kappa > 0.4$) with each annotator in the control group, and (ii) has annotated more than 95% of the ground-truth images as highly relevant.

²https://en.wikipedia.org/wiki/Cohen%27s_kappa#Interpreting_magnitude

Table 1: Statistics about the annotators enrolled in the annotation process for generated images.

Statistic	Min	Mean	Max
#annotations per person	30	1,664	15,045
Fleiss' κ	0.41	0.54	1.00

Annotation interface. We use a custom web interface to collect relevance judgments. The prompts are presented in a random order to each annotator. Each prompt is accompanied by four generated images and one ground-truth image, which are mixed and displayed in a random order, as shown in Figure 2. For each image, annotators are given a choice among four evaluative categories: high relevance, low relevance, no relevance, and unrealistic. Participants receive thorough instructions (summarized below) before starting the annotation process. The ratings are to be assigned as follows: *high relevance* (score 2) – the image depicts over half of the concepts mentioned in the prompt; *low relevance* (score 1) – the image captures at least one concept, but fewer than half; *no relevance* (score 0) – the image is unrelated, yet realistic; *unrealistic* (score -1) – the image exhibits notable artifacts.

Annotation process. Our aim is to collect at least three annotations per image. In order to collect the required number of annotations (10,000 prompts \times 5 images \times 3 annotations = 150,000 annotations in total), we recruit 173 annotators. The annotators providing the relevance judgments are adults having at least a bachelor or college degree. The recruited annotators willingly agreed to engage in the annotation process, after reading our terms and conditions. Annotators are allowed to opt out at any time during the annotation process. To reduce bias or uncertainty, annotators are permitted to update previously made annotations or skip specific prompts altogether. Annotators are informed about the inclusion of control prompts within their tasks, but are not given specifics on the frequency of such prompts. A fair compensation (proportional to the number of annotated prompts) is given to each annotator with a Cohen’s κ coefficient higher than 0.4 on the control prompts. Based on our selection criteria, 26 annotators are excluded from the process. This leaves us with 147 valid annotators. Given the asynchronous nature of the annotation process, several prompts ended up having more than three annotations, leading to a total of 244,650 annotations. When a prompt has more than three relevance judgments, we keep the annotations provided by the top three annotators with the highest Cohen’s κ coefficients (with respect to the control prompts). A brief set of statistics about the enrolled annotators is presented in Table 1. Notably, the Fleiss’ κ coefficient computed across all annotators is consistent with that of the control annotators. Upon excluding the annotations corresponding to the ground-truth images, we find that most images are voted as highly relevant (see Figure 4 in Appendix A.5), confirming that Stable Diffusion and GLIDE generally produce relevant results.

Measuring prompt performance. To derive the final prompt performance in image generation, we first map the relevance categories to numerical values, as follows: *high relevance* is mapped to 2, *low relevance* to 1, *no relevance* to 0, and *unrealistic* to -1.

To exclude outlier annotations, we group the four relevance categories into two high-level categories. The first category, combining the *high relevance* and *low relevance* annotations, represents images that are at least somewhat relevant to the prompt. The second category, combining the *unrealistic* and *no relevance* labels, represents images that are not acceptable for the given prompt, either because they are irrelevant or unrealistic. We hereby acknowledge that the distinction between *high relevance* and *low relevance* is more difficult to determine, involving a fine assessment of how many of the prompt elements are depicted in the image. This requires evaluators to consider not just the presence of these elements, but also their significance and portrayal within the image, making the distinction between high and low relevance inherently more subjective and challenging. In contrast, the distinction between the high-level categories (*relevant* and *irrelevant*) can be easily assessed.

We employ a majority voting mechanism on the high-level categories to decide if a generated image is either *relevant* or *irrelevant*. Since there are only two high level categories and three annotations per image, there is no need to break ties (a majority always exists). The majority voting is performed to rule out outlier annotations. The final relevance of an image is given by averaging the scores (between -1 and 2) associated with the votes forming the majority. The performance of a prompt is given by the average relevance score computed across the four generated images. We further refer to the resulting score as *human-based prompt performance* (HBPP).

3.2 Query Performance Assessment

Retrieval models. For text-to-image retrieval, we employ two distinct vision-language models: CLIP [33] and BLIP-2 [24]. For CLIP, we select the base architecture with patches of 32×32 pixels. For BLIP-2, we choose the ViT-Large [16] backbone. Both models are equipped with the necessary components to perform text-to-image retrieval. These models are pre-trained on natural images, which makes them suitable for image retrieval on MS COCO.

Annotation process. For the retrieval setting, we devise a semi-automatic labeling process to generate reference (ground-truth) relevance judgments for the 10,000 image captions chosen as queries. Limited by the annotation budget, we employ an automatic process to restrict the number of retrieved images to 2,000 per query. We exploit the structure of the MS COCO dataset based on (image, caption) pairs to generate preliminary relevance judgments using sentence BERT [42]. More specifically, we compute the cosine similarity in the embedding space of sentence BERT between each query from the established subset and each caption in MS COCO. Based on a preliminary exploratory data analysis, we set the cosine similarity threshold to 0.7 to determine a comprehensive set of potentially relevant results. The image corresponding to each caption that has the cosine similarity with a query higher than 0.7 is added to the preliminary set of relevant results for the respective query. For some short and generic text queries, the preliminary set may contain thousands of potentially relevant images. For such queries, we refine the results ranked below 1,000 using a bag-of-words representation. More specifically, a low-rank image is kept only if the bag-of-words representation of the query is included in the bag-of-words representation of the aggregated captions of the respective image. All queries are limited to 2,000 images in the preliminary set. The preliminary steps described above generate a total of 1,245,186 images, which are further subject to rigorous manual review. There are 100 annotators involved in the manual annotation of the potentially relevant images. The annotators are asked to label each image as relevant or irrelevant to the corresponding query. Each image is annotated by two annotators. An image is kept in the relevant set if it is voted as relevant by one annotator. Two of the evaluators, who are also the main authors of this paper, annotated a set of 4,000 queries. These 4,000 queries are used as control queries for the other enrolled annotators. The remaining queries were randomly divided into batches of 50 queries. In each batch, there are 5 control queries, which are used to exclude annotators that provide poor relevance judgments. There are 98 human evaluators who annotated between 1 and 4 batches. We employed the F_1 measure on relevant images to estimate the quality of the relevance judgments, and set a threshold of 0.4 to accept annotations. There are 7 annotators who were excluded from the annotation process based on the considered threshold. For the remaining annotators, we obtain a mean F_1 score of 0.727. The minimum F_1 score is 0.447, which is significantly higher than the F_1 score of 0.150 of the random chance baseline. The manual annotation process reduced the total number of relevant images to 431,141. In other words, the annotators removed about a third of the originally retrieved images.

Measuring query performance. To determine the performance level of a query, we employ two alternative measures of retrieval effectiveness, namely the precision for the top n retrieved results ($P@n$) and the reciprocal rank (RR). The precision@ n is the ratio between the number of true positive images and n . Since $P@10$ is often used in text QPP [48], we adopt the same measure and set $n = 10$ for our benchmark. The reciprocal rank of a query is given by the ratio between 1 and the rank of the first relevant result. For example, if the first relevant result is at rank 5, then $RR = 1/5 = 0.2$. We estimate the $P@10$ and RR measures for both CLIP and BLIP-2. Then, the resulting values are averaged across models, thus obtaining an average $P@10$ and an average RR for each query. However, in Appendix A.7, we also report the results per reference system.

3.3 Evaluation Protocol

We divide the annotated prompts/queries into 6,000 for training, 2,000 for validation, and 2,000 for testing. To evaluate performance predictors, we measure the Pearson and Kendall τ correlation coefficients between the predicted and the ground-truth performance levels of all test queries, following conventional evaluation procedures in text [48, 51] and image [32] QPP. Furthermore, we test the significance of the results with respect to the random chance baseline using Student’s t-testing [35].

4 Predictors

4.1 Pre-generation/retrieval Predictors

Basic text predictors. Building on linguistic features to predict query difficulty [29], we extract a comprehensive suite of pre-retrieval linguistic indicators: the diversity of concepts (total WordNet synsets per prompt/query), lexical density (number of words per prompt/query), syntactic complexity (average word length), and the frequency of specific grammatical structures (proper nouns, acronyms, numerals, conjunctions and prepositions). We test a wide variety of basic predictors, but we only report the results of the top three predictors, namely the number of synsets, the number of words, and the frequency of conjunctions.

Fine-tuned BERT. We explore the potential of fine-tuning the BERT model [14] as a pre-retrieval performance predictor. We select the *base* architecture based on cased inputs, since the queries contain named entities. The fine-tuning process involves attaching a custom regression head to the pre-trained BERT backbone, which learns to predict the performance of prompts/queries in image generation and retrieval, respectively. The regression head consists of a dropout layer and two fully connected layers. The dropout rate is set to 0.3 to prevent overfitting. The first dense layer is based on ReLU activation functions, and it takes the [CLS] token returned by BERT and transforms it into a 512-dimensional hidden representation. The second layer contains a single neuron (activated by sigmoid) that predicts prompt/query performance. Before training, the ground-truth performance values are normalized to $[0, 1]$. We employ grid search on the validation set to establish the optimal hyperparameter configuration. More specifically, we consider learning rates between 10^{-3} and 10^{-6} , and weight decays in the set $\{0, 0.1, 0.01\}$. All versions are trained for 15 epochs with early stopping, on mini-batches of 256 samples. We employ AdamW and optimize the mean squared error (MSE) loss. The fine-tuning is independently carried out for the two tasks, generation and retrieval.

4.2 Post-generation/retrieval Predictors

Fine-tuned CLIP. Our first post-generation/retrieval predictor is based on fine-tuning a CLIP model on (query, image) pairs. We attach a regression head for the image generation scenario, and a binary classification head for the image retrieval scenario. The utilization of CLIP-based embeddings is aimed at leveraging the model’s capacity to jointly represent text and image modalities in a single latent space. The fine-tuned CLIP learns to predict the relevance judgment of each generated or retrieved image for a given prompt/query. The performance of the prompt/query is then predicted by aggregating the predicted relevance judgments. For the generative task, the model uses all four images generated by Stable Diffusion and GLIDE. For the retrieval task, we limit the training data to the first 25 images returned by each retrieval model. Although 10 images would be enough for the P@10 metric, estimating the RR measure can require more images. A statistical analysis of the training queries indicates that more than 95% of the queries have the first relevant image at a rank higher than 25, which motivates our choice for limiting the training data to 25 images per model. The regression/classification head is composed of a two-layer neural network of 512 and 256 neurons, respectively. Both layers are based on ReLU activations. A dropout layer with a drop rate of 0.5 is added after each dense layer. For the generative task, another layer comprising a single neuron is added to predict prompt performance. The objective of the model is to minimize the MSE loss. For the retrieval task, the last neuron has to determine if an input (query, image) pair is relevant or irrelevant. This is a binary classification task, so the model is trained via binary cross-entropy. We perform a grid search to find the best hyperparameters, considering learning rates between 10^{-3} and 10^{-6} , and weight decays in the set $\{0, 0.1, 0.01\}$. We employ the AdamW optimizer for 25 epochs with early stopping, using a batch size of 256.

Correlation-based CNN. Following the work of Sun et al. [41], we employ a convolutional neural network (CNN) trained on the set of generated or retrieved images, respectively. The CNN model takes a correlation matrix between all image pairs as input. For the generative task, the size of the input correlation matrix is 4×4 . For the retrieval task, we apply the same limit to the number of retrieved images per query as for the fine-tuned CLIP predictor. Hence, the size of the correlation matrix for one retrieval model is 25×25 . We concatenate the correlation matrices for CLIP and BLIP-2 models in the channel dimension, which results in a tensor of $25 \times 25 \times 2$ components, that is given as input to the CNN. The correlation of an (image, image) pair is given by the cosine similarity between the (pre-trained) CLIP embeddings of the respective images. The CNN architecture is composed of four convolutional-pooling blocks, followed by two linear layers. This is a custom

Table 2: Results of the prompt/query performance predictors for the generative and retrieval settings on the test set. On the generative task, we report the correlation of the predicted value with the average HBPP performance of Stable Diffusion and GLIDE. On the retrieval task, the correlation is computed for the average P@10 and the average RR, where the averages are computed over CLIP and BLIP-2. For each task, the highest correlation is highlighted in bold. According to a Student’s t-test, the results marked with † and ‡ are significantly better than the random chance baseline at p-values 0.01 and 0.001, respectively. Detailed results for each model are in Appendix A.7.

Predictor Type	Predictor Name	Generative Task		Retrieval Task			
		HBPP		P@10		RR	
		Pearson	Kendall	Pearson	Kendall	Pearson	Kendall
Pre-	#synsets	-0.152 [‡]	-0.093 [‡]	-0.141 [‡]	-0.097 [‡]	-0.071 [†]	-0.037 [†]
	#words	-0.136 [‡]	-0.113 [‡]	-0.199 [‡]	-0.163 [‡]	-0.069 [†]	-0.052 [†]
	#conjunctions / #words	0.058 [†]	0.045 [†]	-0.117 [‡]	-0.097 [‡]	-0.041	-0.040
	Fine-tuned BERT	0.568 [‡]	0.416 [‡]	0.507[‡]	0.318 [‡]	0.262 [‡]	0.182 [‡]
Post-	Fine-tuned CLIP	0.600[‡]	0.448[‡]	0.490 [‡]	0.330[‡]	0.197 [‡]	0.129 [‡]
	Correlation CNN	0.471 [‡]	0.347 [‡]	0.327 [‡]	0.196 [‡]	0.301[‡]	0.212[‡]

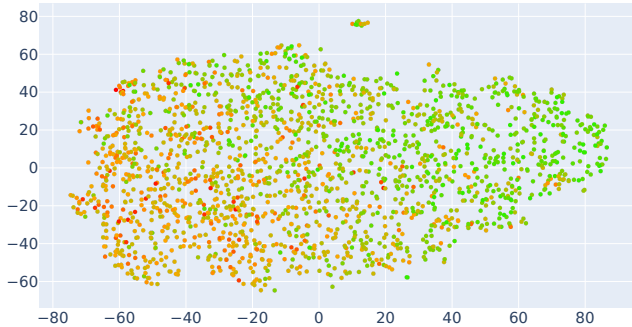


Figure 3: t-SNE visualization of the test prompts embedded in the latent space of the fine-tuned BERT on the generation task. The ground-truth HBPP performance is encoded via a color map from green to red. The visualization confirms that the fine-tuned BERT predictor learns a meaningful representation of the prompts. Best viewed in color.

architecture that comprises 3×3 convolutional filters applied at a stride of 1, using a padding of 1. The number of filters in each of the four convolutional layers is 64, 128, 256 and 512, respectively. A max-pooling is applied after each convolutional layer. The pooling operation uses 2×2 filters applied at a stride of 2. The first fully connected layer comprises 1024 units. Each hidden neuron is followed by a ReLU activation. The final layer comprises a single neuron that is trained in a regression setting via the MSE loss. The hyperparameter tuning is identical to the one employed for the fine-tuned CLIP model. The correlation-based CNN is trained for 25 epochs using AdamW with early stopping, on mini-batches of 256 samples.

5 Experiments and Results

In Table 2, we report the results of the established predictors for both generative and retrieval tasks, where the reference or ground truth is the average of the two reference systems. We provide the separate results for each reference system in Appendix A.7. For the generative task, the highest correlation between the predicted and the actual performance corresponds to the fine-tuned CLIP, with a Pearson correlation coefficient of 0.6. This predictor shows a lower correlation with P@10 in the retrieval task, where the Pearson score is 0.49. In general, predictors exhibit higher correlations with HBPP than with P@10. The best predictor among the pre-generation/retrieval ones is the fine-tuned BERT, for both tasks and all evaluation measures. Its correlation measures clearly indicate a positive correlation, e.g. the Pearson correlation with P@10 on the retrieval task is as high as 0.507. The two post-generation/retrieval predictors exhibit good performance levels. The fine-tuned CLIP provides better results for the HBPP and P@10 measures, while the correlation CNN is more suitable for the

RR measure. Overall, an interesting finding of our study is that the pre-retrieval fine-tuned BERT is a worthy competitor for the better post-retrieval predictor (fine-tuned CLIP). In Table 2, we only report the predictors that obtain a correlation higher than 0.1, in at least one evaluation scenario. The results of the full set of predictors are presented in Appendix A.7. The very limited effectiveness of the excluded pre-generation/retrieval predictors can be attributed to their behavior of capturing only a limited portion of the relevant information (see also Appendix A.6).

In Figure 3, we present a t-SNE visualization of the test prompts embedded in the latent space of the BERT predictor fine-tuned on the generation task. We observe that the learned embedding correlates well with the ground-truth HBPP values, explaining the high accuracy of the fine-tuned BERT predictors on the generation task. An analogous visualization for the retrieval task is shown in Figure 6 from Appendix A.8.

Additional results. In Appendix A.6, we discuss empirical evidence regarding the overlap between generation and retrieval performance. In Appendix A.7, we present the complete set of quantitative results. In Appendix A.8, we analyze the generation/retrieval results from a qualitative perspective.

6 Conclusion and Future Work

Benchmark collections lay the grounds for the development of effective approaches to solve new challenges. In this paper, we have developed the first manually-labeled benchmark for prompt performance prediction in the context of prompt-to-image generation. Our benchmark is also applicable for query-to-image retrieval, enabling the direct comparison of the performance prediction task in generation vs. retrieval scenarios. Our dataset and code are made publicly available to the research community.

One direction for future work is to develop a model that combines different pre-retrieval predictors. Combining predictors in a supervised manner has shown its effectiveness in text [13] and image [32] QPP. Another important direction is to organize a shared task associated with the proposed PQPP benchmark, so that the IR community can further explore the novel task of prompt performance prediction in image generation.

References

- [1] Qingyao Ai, Ting Bai, Zhao Cao, Yi Chang, Jiawei Chen, Zhumin Chen, Zhiyong Cheng, Shoubin Dong, Zhicheng Dou, Fuli Feng, Shen Gao, Jiafeng Guo, Xiangnan He, Yanyan Lan, Chenliang Li, Yiqun Liu, Ziyu Lyu, Weizhi Ma, Jun Ma, Zhaochun Ren, Pengjie Ren, Zhiqiang Wang, Mingwen Wang, Ji-Rong Wen, Le Wu, Xin Xin, Jun Xu, Dawei Yin, Peng Zhang, Fan Zhang, Weinan Zhang, Min Zhang, and Xiaofei Zhu. Information Retrieval meets Large Language Models: A strategic report from Chinese IR community. *AI Open*, 4:80–90, 2023.
- [2] Negar Arabzadeh, Fattane Zarrinkalam, Jelena Jovanovic, and Ebrahim Bagheri. Neural embedding-based metrics for pre-retrieval query performance prediction. In *Proceedings of ECIR*, pages 78–85. Springer, 2020.
- [3] Negar Arabzadeh, Maryam Khodabakhsh, and Ebrahim Bagheri. Bert-qpp: contextualized pre-trained transformers for query performance prediction. In *Proceedings of CIKM*, pages 2857–2861, 2021.
- [4] Nicolas Bizzozzero, Ihab Bendidi, and Olivier Risser-Maroux. Prompt performance prediction for generative ir. *arXiv preprint arXiv:2306.08915*, 2023.
- [5] Kevin Matthe Caramancion. Large Language Models vs. Search Engines: Evaluating User Preferences Across Varied Information Retrieval Scenarios. *arXiv preprint arXiv:2401.05761*, 2024.
- [6] David Carmel and Elad Yom-Tov. Estimating the query difficulty for information retrieval. *Synthesis Lectures on Information Concepts, Retrieval, and Services*, 2(1):1–89, 2010.
- [7] Florinel-Alin Croitoru, Vlad Hondru, Radu Tudor Ionescu, and Mubarak Shah. Diffusion Models in Vision: A Survey. *IEEE Transactions on Pattern Analysis and Machine Intelligence*, 45(9):10850–10869, 2023.

- [8] Steve Cronen-Townsend, Yun Zhou, and W. Bruce Croft. Predicting query performance. In *Proceedings of SIGIR*, pages 299–306, 2002.
- [9] Ronan Cummins, Joemon Jose, and Colm O’Riordan. Improved query performance prediction using standard deviation. In *Proceedings of SIGIR*, pages 1089–1090, 2011.
- [10] Suchana Datta, Debasis Ganguly, Derek Greene, and Mandar Mitra. Deep-QPP: A pairwise interaction-based deep learning model for supervised query performance prediction. In *Proceedings of WSDM*, pages 201–209, 2022.
- [11] Suchana Datta, Debasis Ganguly, Josiane Mothe, and Md Zia Ullah. Combining Word Embedding Interactions and LETOR Feature Evidences for Supervised QPP. In *Proceedings of QPP++*, volume 3366, pages 7–12, 2023.
- [12] Claude De Loupy and Patrice Bellot. Evaluation of document retrieval systems and query difficulty. In *Proceedings of LREC*, pages 32–39, 2000.
- [13] Sébastien Déjean, Radu Tudor Ionescu, Josiane Mothe, and Md Zia Ullah. Forward and backward feature selection for query performance prediction. In *Proceedings of SAC*, pages 690–697, 2020.
- [14] Jacob Devlin, Ming-Wei Chang, Kenton Lee, and Kristina Toutanova. BERT: Pre-training of Deep Bidirectional Transformers for Language Understanding. In *Proceedings of NAACL*, pages 4171–4186, 2019.
- [15] Prafulla Dhariwal and Alexander Nichol. Diffusion models beat GANs on image synthesis. In *Proceedings of NeurIPS*, volume 34, pages 8780–8794, 2021.
- [16] Alexey Dosovitskiy, Lucas Beyer, Alexander Kolesnikov, Dirk Weissenborn, Xiaohua Zhai, Thomas Unterthiner, Mostafa Dehghani, Matthias Minderer, Georg Heigold, Sylvain Gelly, Jakob Uszkoreit, and Neil Houlsby. An image is worth 16x16 words: Transformers for image recognition at scale. In *Proceedings of ICLR*, 2021.
- [17] Guglielmo Faggioli, Oleg Zendel, J Shane Culpepper, Nicola Ferro, and Falk Scholer. smare: a new paradigm to evaluate and understand query performance prediction methods. *Information Retrieval Journal*, 25(2):94–122, 2022.
- [18] Guglielmo Faggioli, Thibault Formal, Stefano Marchesin, Stéphane Clinchant, Nicola Ferro, and Benjamin Piwowarski. Query performance prediction for neural ir: Are we there yet? In *Proceedings of ECIR*, pages 232–248, 2023.
- [19] Helia Hashemi, Hamed Zamani, and W. Bruce Croft. Performance prediction for non-factoid question answering. In *Proceedings of SIGIR*, pages 55–58, 2019.
- [20] Claudia Hauff, Djoerd Hiemstra, and Franciska de Jong. A survey of pre-retrieval query performance predictors. In *Proceedings of CIKM*, pages 1419–1420, 2008.
- [21] Claudia Hauff, Leif Azzopardi, and Djoerd Hiemstra. The combination and evaluation of query performance prediction methods. In *Proceedings of ECIR*, pages 301–312, 2009.
- [22] Ben He and Iadh Ounis. Inferring query performance using pre-retrieval predictors. In *Proceedings of SPIRE*, pages 43–54, 2004.
- [23] Nupur Kumari, Bingliang Zhang, Sheng-Yu Wang, Eli Shechtman, Richard Zhang, and Jun-Yan Zhu. Ablating concepts in text-to-image diffusion models. In *Proceedings of ICCV*, pages 22691–22702, 2023.
- [24] Junnan Li, Dongxu Li, Silvio Savarese, and Steven Hoi. BLIP-2: Bootstrapping Language-Image Pre-training with Frozen Image Encoders and Large Language Models. In *Proceedings of ICML*, pages 19730–19742. PMLR, 2023.
- [25] Yangxi Li, Bo Geng, Linjun Yang, Chao Xu, and Wei Bian. Query difficulty estimation for image retrieval. *Neurocomputing*, 95:48–53, 2012.

- [26] Tsung-Yi Lin, Michael Maire, Serge Belongie, James Hays, Pietro Perona, Deva Ramanan, Piotr Dollár, and Lawrence C. Zitnick. Microsoft COCO: Common Objects in Context. In *Proceedings of ECCV*, pages 740–755, 2014.
- [27] Chuan Meng, Negar Arabzadeh, Mohammad Aliannejadi, and Maarten de Rijke. Query performance prediction: From ad-hoc to conversational search. In *Proceedings of SIGIR*, pages 2583–2593, 2023.
- [28] Josiane Mothe. On Correlation to Evaluate QPP. In *Proceedings of QPP++*, volume 3366, pages 29–36, 2023.
- [29] Josiane Mothe and Ludovic Tanguy. Linguistic features to predict query difficulty. In *Proceedings of SIGIR*, pages 7–10, 2005.
- [30] Alex Nichol, Prafulla Dhariwal, Aditya Ramesh, Pranav Shyam, Pamela Mishkin, Bob McGrew, Ilya Sutskever, and Mark Chen. GLIDE: Towards Photorealistic Image Generation and Editing with Text-Guided Diffusion Models. In *Proceedings of ICML*, pages 16784–16804, 2021.
- [31] Nikita Pavlichenko and Dmitry Ustalov. Best prompts for text-to-image models and how to find them. In *Proceedings of SIGIR*, pages 2067–2071, 2023.
- [32] Eduard Poesina, Radu Tudor Ionescu, and Josiane Mothe. iQPP: A Benchmark for Image Query Performance Prediction. In *Proceedings of SIGIR*, pages 2953–2963, 2023.
- [33] Alec Radford, Jong Wook Kim, Chris Hallacy, Aditya Ramesh, Gabriel Goh, Sandhini Agarwal, Girish Sastry, Amanda Askell, Pamela Mishkin, Jack Clark, Gretchen Krueger, and Ilya Sutskever. Learning Transferable Visual Models From Natural Language Supervision. In *Proceedings of ICML*, pages 8748–8763, 2021.
- [34] Fiana Raiber and Oren Kurland. Query-performance prediction: setting the expectations straight. In *Proceedings of SIGIR*, pages 13–22, 2014.
- [35] Haggai Roitman. An extended query performance prediction framework utilizing passage-level information. In *Proceedings of SIGIR*, pages 35–42, 2018.
- [36] Robin Rombach, Andreas Blattmann, Dominik Lorenz, Patrick Esser, and Björn Ommer. High-Resolution Image Synthesis with Latent Diffusion Models. In *Proceedings of CVPR*, pages 10684–10695, 2022.
- [37] Mohammadreza Samadi and Davood Rafiei. Performance Prediction for Multi-hop Questions. *arXiv preprint arXiv:2308.06431*, 2023.
- [38] Anna Shtok, Oren Kurland, David Carmel, Fiana Raiber, and Gad Markovits. Predicting query performance by query-drift estimation. *ACM Transactions on Information Systems*, 30(2):1–35, 2012.
- [39] Ashutosh Singh, Debasis Ganguly, Suchana Datta, and Craig McDonald. Unsupervised query performance prediction for neural models with pairwise rank preferences. In *Proceedings of SIGIR*, pages 2486–2490, 2023.
- [40] Karen Sparck Jones. A statistical interpretation of term specificity and its application in retrieval. *Journal of Documentation*, 28(1):11–21, 1972.
- [41] Shaoyan Sun, Wengang Zhou, Qi Tian, Ming Yang, and Houqiang Li. Assessing image retrieval quality at the first glance. *IEEE Transactions on Image Processing*, 27(12):6124–6134, 2018.
- [42] Nandan Thakur, Nils Reimers, Johannes Daxenberger, and Iryna Gurevych. Augmented SBERT: Data Augmentation Method for Improving Bi-Encoders for Pairwise Sentence Scoring Tasks. In *Proceedings of NAACL*, pages 296–310, 2021.
- [43] Xinmei Tian, Yijuan Lu, and Linjun Yang. Query difficulty prediction for web image search. *IEEE Transactions on Multimedia*, 14(4):951–962, 2011.
- [44] Xinmei Tian, Qianghuai Jia, and Tao Mei. Query difficulty estimation for image search with query reconstruction error. *IEEE Transactions on Multimedia*, 17(1):79–91, 2014.

- [45] Lucas Pascotti Valem, Vanessa Helena Pereira-Ferrero, and Daniel Carlos Guimarães Pedronette. Self-supervised regression for query performance prediction on image retrieval. In *Proceedings of AIKE*, pages 95–98. IEEE, 2023.
- [46] Xiaoshi Wu, Keqiang Sun, Feng Zhu, Rui Zhao, and Hongsheng Li. Human preference score: Better aligning text-to-image models with human preference. In *Proceedings of ICCV*, pages 2096–2105, 2023.
- [47] Xing Xing, Yi Zhang, and Mei Han. Query difficulty prediction for contextual image retrieval. In *Proceedings of ECIR*, pages 581–585. Springer, 2010.
- [48] Elad Yom-Tov, Shai Fine, David Carmel, and Adam Darlow. Learning to estimate query difficulty: including applications to missing content detection and distributed information retrieval. In *Proceedings of SIGIR*, pages 512–519, 2005.
- [49] Hamed Zamani, W. Bruce Croft, and J. Shane Culpepper. Neural query performance prediction using weak supervision from multiple signals. In *Proceedings of SIGIR*, pages 105–114, 2018.
- [50] Zhongmin Zhang, Jiawei Chen, and Shengli Wu. Query performance prediction and classification for information search systems. In *Proceedings of APWeb-WAIM*, pages 277–285, 2018.
- [51] Ying Zhao, Falk Scholer, and Yohannes Tsegay. Effective pre-retrieval query performance prediction using similarity and variability evidence. In *Proceedings of ECIR*, pages 52–64. Springer, 2008.
- [52] Yun Zhou and W. Bruce Croft. Query performance prediction in web search environments. In *Proceedings of SIGIR*, pages 543–550. ACM, 2007.
- [53] Yutao Zhu, Huaying Yuan, Shuting Wang, Jiongnan Liu, Wenhan Liu, Chenlong Deng, Zhicheng Dou, and Ji-Rong Wen. Large language models for information retrieval: A survey. *arXiv preprint arXiv:2308.07107*, 2023.

A Appendix

A.1 Limitations

We recognize specific limitations in the annotation processes for both generative and retrieval tasks. In the generative setting, prompts can be subjectively interpreted by users, which may introduce variability in the results. To mitigate this, we incorporated a control set, excluded annotations from annotators who failed on the control set, and computed an average score from multiple user annotations for each image/prompt pair, enhancing the robustness of the evaluations.

In the retrieval setting, the initial ground-truth image bank was generated using a method that combines Sentence-BERT and the bag-of-words model. We acknowledge that some images may contain content that is not fully or accurately captured by their paired captions, which could introduce occasional false negatives or false positives in the ground-truth collection. This heuristic was chosen to minimize the number of false negatives, while the false positives were mostly curated by the enrolled annotators.

Another limitation of our study is that we consider prompts that correspond to naturally occurring images. However, generative models are often used to generate fictive images. Since retrieval models can only retrieve images from a database of real images, queries that correspond to fictive images can be easily labeled as difficult. We therefore choose captions from MS COCO to serve as prompts/queries for our benchmark, creating an evaluation setting that is representative for both generation and retrieval.

A.2 Potential Negative Societal Impact

The development and deployment of text-to-image generation and retrieval systems come with several societal implications that warrant careful consideration. Here, we outline key areas of concern. Our

enhanced dataset is built upon a preexisting large dataset, which may inherit and perpetuate biases present in the original data. Additionally, user annotations might have been influenced by their own cultural backgrounds, potentially introducing subjective biases into the final decisions. The pre-trained generative models employed in our study could also exhibit inherent biases, affecting the generated outputs. These combined factors could lead to unfair representations or reinforce existing stereotypes. We acknowledge the necessity of ongoing efforts to identify, measure, and mitigate these biases to ensure the fairness and inclusiveness of our models. In our work, we address these concerns by promoting transparency in our methodology and unifying multiple user annotations to mitigate possible individual biases.

The computational resources required for data collection, filtering, and model training contribute to energy consumption and carbon emissions. We recognize the environmental impact of our work and emphasize the importance of optimizing computational processes and exploring sustainable practices to reduce the ecological footprint of AI research.

Moreover, our benchmark can be used to develop and improve generative models. Such models can further be used in unethical scenarios, e.g. to generate deep fakes. In recent years, an increase in deep fake materials flooded the web, either to spread false information or to steal sensitive information by impersonating trustworthy individuals. While we strongly believe in the benefits of very capable generative models, we are aware of the potential risks. However, we can see that governments are working very closely with academia and industry on safely developing artificial intelligence, and thus observe and support the increasing focus on models that detect AI-generated content to mitigate the aforementioned risks.

A.3 Ethical Considerations on Data Annotation

Data annotation by students is a common practice in our three universities (University of Bucharest, Aix-Marseille Université, Université Toulouse Jean-Jaurès) and we followed the standard protocols to get approvals from the corresponding ethics committees. The enrolled students were compensated with bonus points. We would like to emphasize that the students understood that the annotation task is optional, and they could also get the extra bonus points by performing alternative tasks (which did not involve data annotation). Moreover, all students were given the opportunity to obtain a full grade without the optional annotation task. Hence, there was no obligation for any of the students to perform the annotations. The students were also able to opt out, at any time during the annotation, without any penalties.

The enrolled students come from three universities from two different countries (France and Romania). They represent different cultural, gender and age groups, reflecting the varied distribution of students in each of the three universities.

A.4 Related Work on QPP in Text Retrieval

Pre-retrieval features are based on information available prior to the execution of the query. Some are independent to the document collection, such as query length, part-of-speech features (including the number of words of some grammatical categories), query ambiguity [12], and query complexity [29]. Other pre-retrieval features depend on the document collection statistics, such as the inverse document frequency [40], the query scope [22] (which measures the coverage of a query within the context of a document collection and estimates the proportion of documents that are relevant to the query), and the SQC [51] (which is a similarity score between the query and the collection). Pre-retrieval predictors have the huge advantage of being determined before running the search, but they have been found to be less effective than post-retrieval ones on textual ad hoc retrieval [20, 29, 34, 38]. Unlike pre-retrieval features, post-retrieval features require conducting document retrieval with the query. Most of these features are calculated based on the scores of the retrieved documents, quantifying the robustness of the document list, or considering the distribution of the document scores [6, 8, 9, 34, 50]. On textual IR, the Clarity Score estimates the specificity of a query considering the language distribution of the document collection and that of the top-retrieved documents [8]. The Normalized Query Commitment (NQC), also known as the query drift [38], measures how much the retrieved documents deviate from the central topic of the query. The Weighted Information Gain (WIG) calculates the difference in information content between the documents retrieved for a specific query and a baseline distribution of information in the collection or corpus, based on the scores of the top-retrieved documents [52].



Figure 4: A histogram showing the number of annotations per category for images generated by Stable Diffusion XL and GLIDE.

Table 3: Pearson and Kendall τ correlation coefficients between the performance levels measured in image generation vs. image retrieval. According to a Student’s t-test, the results marked with \dagger and \ddagger are significantly better than the random chance baseline at p-values 0.01 and 0.001, respectively.

Metric	Pearson	Kendall
HBPP vs. P@10	0.118 \ddagger	0.082 \ddagger
HBPP vs. RR	0.070 \ddagger	0.046 \dagger
P@10 vs. RR	0.562 \ddagger	0.504 \ddagger

The main conclusions from the earlier studies on QPP for textual ad hoc retrieval are that post-retrieval predictors outperform pre-retrieval ones [34], and combinations of predictors using supervised approaches are the most effective [13].

More recent work investigated QPP on neural IR (NIR) systems [2, 10, 18, 27, 39, 49]. Datta et al. [10] employed convolutional neural layers for their Deep-QPP predictor. This architecture has further been combined with LETOR post-retrieval predictors with some success [11]. According to Faggioli et al. [18], QPP models which have been developed for sparse IR methods perform worse when applied to NIR systems. However, the authors did not consider linguistic-based predictors in their work. On the other hand, supervised BERT-based QPP models seem to work better. Arabzadeh et al. [3] used BERT to predict the performance of search queries in terms of their ability to retrieve relevant documents from a corpus. Such predictors may better capture the semantic aspects of the query-document matching.

Other recent studies focused on the transition from ad hoc search to conversational search [27] or question answering [19, 37]. In conversational search, the experiments showed that supervised QPP methods outperform unsupervised ones when a large amount of training data is available, but unsupervised methods are effective in conversational dense retrieval method assessment.

A.5 Distribution of Human Relevance Judgments for Prompt Performance Prediction

In Figure 4, we show the number of annotations per category label computed for the four images generated for each prompt. Although the annotations corresponding to the ground-truth images are excluded, it is clear that most images are voted as highly relevant, confirming that Stable Diffusion and GLIDE generally produce relevant results.

A.6 Generation vs. Retrieval Performance

For each query, our benchmark provides performance measurements in both generation and retrieval settings. Taking advantage of the structure of the PQPP benchmark, we next analyze the correlation between the studied tasks: prompt performance prediction (in text-to-image generation) and query performance prediction (in text-to-image retrieval). We present the correlation results in Table 3.

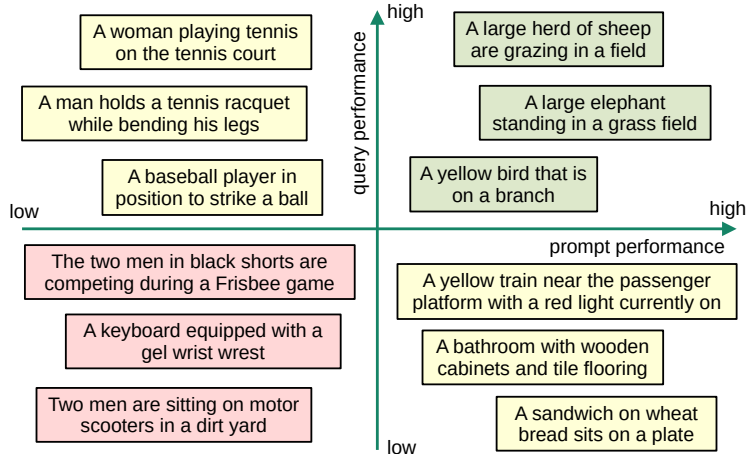


Figure 5: Representative prompts/queries that exhibit high or low performance in text-to-image generation (on the horizontal axis) and text-to-image retrieval (on the vertical axis).

Although the correlations are statistically significant, the empirical analysis reveals surprisingly low correlations between the ground-truth performance measurements for the generative and retrieval tasks. This observation indicates that the tasks are rather orthogonal, confirming that image generation requires the development of dedicated prompt performance predictors.

Aside from the quantitative results presented in Table 3, we manually inspect prompts/queries from the following four categories: (1) high performance in both generation and retrieval; (2) high performance in generation, low performance in retrieval; (3) low performance in generation, high performance in retrieval; and (4) low performance in both generation and retrieval. We present illustrative captions of the four categories in Figure 5. For the first category, the queries usually refer to an animate object performing an action in a location. There are no or few attributes to describe the objects or the location, which increases the likelihood of finding many matches during retrieval, and reduces the constraints during generation. The queries from the second category include inanimate objects with specific descriptions. Generative models seem to handle many specific attributes rather well, but the retrieval models have a hard time finding images that match the specific descriptions. The third category comprises queries about a person performing an action specific to some sport. The MS COCO database contains many images of people playing sports, which makes the retrieval task pretty easy. However, generative models struggle to generate a person in a specific pose, performing a certain action that typically involves interacting with an object, e.g. tennis racket or baseball bat. For the fourth category, representative queries refer to groups of people, e.g. two men, performing specific actions in specific locations, which are rather uncommon. Queries in this category can also refer to uncommon objects with specific attributes, which can even be misspelled, e.g. “gel wrist wrest”. Prompts/queries describing rare situations/objects are difficult for both generative and retrieval models. On the one hand, there is some common ground between prompt/query performance in generation and retrieval, as confirmed by the examples from the first and fourth categories. On the other hand, the examples from the second and third categories indicate that there are task-specific characteristics placing prompt and query performance prediction at opposite poles. Therefore, we conclude that the task of prompt performance prediction merits further investigation, motivating the utility of our novel benchmark.

A.7 Detailed Quantitative Results

In Table 4, we present the results of prompt performance predictors for each generative model (Stable Diffusion and GLIDE). We observe that predicting prompt performance for Stable Diffusion is generally more difficult than for GLIDE. This observation can be attributed to the higher variety (in terms of relevance to the prompt) of the images generated by GLIDE.

In Table 5 and Table 6, we report the results of query performance predictors for the CLIP and BLIP-2 retrieval systems, respectively. The results are consistent with the ones presented in Table 2, which are obtained by averaging the performance of the two models as a ground truth. Indeed, the

Table 4: Results of the prompt performance predictors for the generative setting on the test set. We report the correlation of the predicted value with the HBPP performance for Stable Diffusion and GLIDE, respectively. For each generative model, the highest correlation is highlighted in bold. According to a Student’s t-test, the results marked with † and ‡ are significantly better than the random chance baseline at p-values 0.01 and 0.001, respectively.

Predictor Type	Predictor Name	Generative Task			
		Stable Diffusion		GLIDE	
		Pearson	Kendall	Pearson	Kendall
Pre-	#synsets	-0.115 [‡]	-0.085 [‡]	-0.123 [‡]	-0.082 [‡]
	#words	-0.118 [‡]	-0.115 [‡]	-0.101 [‡]	-0.092 [‡]
	#conjunctions / #words	0.037	-0.011	0.051	0.041
	Fine-tuned BERT	0.252[‡]	0.149[‡]	0.558 [‡]	0.405 [‡]
Post-	Fine-tuned CLIP	0.247 [‡]	0.141 [‡]	0.615[‡]	0.461[‡]
	Correlation CNN	0.158 [‡]	0.061 [‡]	0.505 [‡]	0.368 [‡]

Table 5: Results of the query performance predictors for the retrieval setting on the test set. The correlation is computed for the P@10 and RR scores of CLIP. For each measure and retrieval system, the highest correlation is highlighted in bold. According to a Student’s t-test, the results marked with † and ‡ are significantly better than the random chance baseline at p-values 0.01 and 0.001, respectively.

Predictor Type	Predictor Name	Retrieval Task (CLIP)			
		P@10		RR	
		Pearson	Kendall	Pearson	Kendall
Pre-	#synsets	-0.129 [‡]	-0.080 [‡]	-0.052	-0.035
	#words	-0.161 [‡]	-0.132 [‡]	-0.054	-0.053
	#conjunctions / #words	-0.086 [‡]	-0.073 [‡]	-0.029	-0.029
	Fine-tuned BERT	0.441 [‡]	0.272 [‡]	0.218 [‡]	0.157 [‡]
Post-	Fine-tuned CLIP	0.458[‡]	0.299[‡]	0.173 [‡]	0.120 [‡]
	Correlation CNN	0.314 [‡]	0.180 [‡]	0.279[‡]	0.210[‡]

pre-retrieval predictors based on the number of synsets, the number of words, and the ratio between conjunctions and words are weakly correlated with the individual system performance. For the RR performance measure, both Pearson and Kendall correlations indicate that the best predictor for both retrieval models is the correlation CNN. For P@10, the correlation for the pre-retrieval fine-tuned BERT and the post-retrieval fine-tuned CLIP are very close to each other, for both retrieval models and both correlation measures.

In Table 7, we present the results for all the considered predictors, although as mentioned in Section 5, Table 2 shows the most interesting predictors. It is nevertheless important to also report failed attempts on specific predictors. In general, we find that neural predictors clearly outperform predictors that are based on simple heuristics.

A.8 Qualitative Results

In Figure 6, we present a t-SNE visualization of the test queries embedded in the latent space of the BERT predictor fine-tuned on the retrieval task. We observe that the learned embedding correlates well with the ground-truth P@10 values, explaining the high accuracy of the fine-tuned BERT predictor on the retrieval task. The separation between easy and difficult queries is evident in the retrieval setting, which is consistent with the quantitative results reported in Table 2, where the fine-tuned BERT exhibits generally higher Pearson and Kendall τ correlation coefficients with P@10 than with HBPP.

In Figure 7, we illustrate the correlation between the HBPP scores predicted by the post-generation fine-tuned CLIP predictor and the ground-truth HBPP scores, via box plots. In this image generation

Table 6: Results of the query performance predictors for the retrieval setting on the test set. The correlation is computed for the P@10 and RR scores of BLIP-2. For each measure and retrieval system, the highest correlation is highlighted in bold. According to a Student’s t-test, the results marked with † and ‡ are significantly better than the random chance baseline at p-values 0.01 and 0.001, respectively.

Predictor Type	Predictor Name	Retrieval Task (BLIP-2)			
		P@10		RR	
		Pearson	Kendall	Pearson	Kendall
Pre-	#synsets	-0.134‡	-0.095‡	-0.063†	-0.036
	#words	-0.206‡	-0.167‡	0.058†	0.042‡
	#conjunctions / #words	-0.128‡	-0.108‡	-0.038	-0.039
	Fine-tuned BERT	0.499‡	0.317‡	0.210‡	0.157‡
Post-	Fine-tuned CLIP	0.457‡	0.339‡	0.149‡	0.115‡
	Correlation CNN	0.298‡	0.190‡	0.213‡	0.160‡

Table 7: Complete results of the prompt/query performance predictors for the generative and retrieval settings on the test set. On the generative task, we report the correlation of the predicted value with the average HBPP performance of Stable Diffusion and GLIDE. On the retrieval task, the correlation is computed for the average P@10 and the average RR, where the averages are computed over CLIP and BLIP-2. For each task, the highest correlation is highlighted in bold. According to a Student’s t-test, the results marked with † and ‡ are significantly better than the random chance baseline at p-values 0.01 and 0.001, respectively.

Predictor Type	Predictor Name	Generative Task		Retrieval Task			
		HBPP		P@10		RR	
		Pearson	Kendall	Pearson	Kendall	Pearson	Kendall
Pre-	#synsets	-0.152‡	-0.093‡	-0.141‡	-0.097‡	-0.071†	-0.037†
	#words	-0.136‡	-0.113‡	-0.199‡	-0.163‡	-0.069†	-0.052†
	avg word length	0.049	0.039†	-0.116‡	-0.084‡	-0.067†	-0.046†
	avg #acronyms	0.010	0.004	-0.001	-0.021	0.015	0.012
	avg #numerals	-0.045	-0.036	-0.065†	-0.066‡	-0.018	-0.001
	#conjunctions / #words	0.058†	0.045†	-0.117‡	-0.097‡	-0.041	-0.040
	#prepositions / #words	0.032	0.013	0.060†	0.034	0.035	0.024
	edge count	0.037	0.062‡	0.027	0.047	0.013	0.010
	edge weight sum	0.030	0.057‡	0.025	0.046†	0.018	0.004
	inverse weight freq	0.090‡	0.071‡	0.045	0.039	0.010	0.011
	degree centrality	0.027	0.005	0.008	0.030	0.028	0.001
	cloneness centrality	0.085‡	0.065‡	0.048	0.038	0.016	0.011
	between centrality	0.020	0.004	0.007	0.016	0.020	0.004
	Page Rank	0.086	0.064	0.049	0.040†	0.014	0.011
	Fine-tuned BERT	0.568‡	0.416‡	0.507‡	0.318‡	0.262‡	0.182‡
Post-	Fine-tuned CLIP	0.600‡	0.448‡	0.490‡	0.330‡	0.197‡	0.129‡
	Correlation CNN	0.471‡	0.347‡	0.327‡	0.196‡	0.301‡	0.212‡
	Score Variance @100	0.003	0.005	0.016	0.003	0.016	0.004

setting, the model does not seem capable of distinguishing between prompts with *unrealistic* (score -1) and *irrelevant* (score 0) images (left-hand side of the figure). In contrast, there is a more obvious correlation between prompts with *irrelevant* (score 0), *lowly relevant* (score 1) and *highly relevant* (score 2) images (right-hand side of the figure). An analogous plot for the retrieval task is displayed in Figure 8, where the comparison is based on the fine-tuned BERT the P@10 measure. In the image retrieval setting, the box plots indicate that the fine-tuned BERT exhibits low variance for low P@10 values. However, queries with high difficulty are not handled well by this predictor.

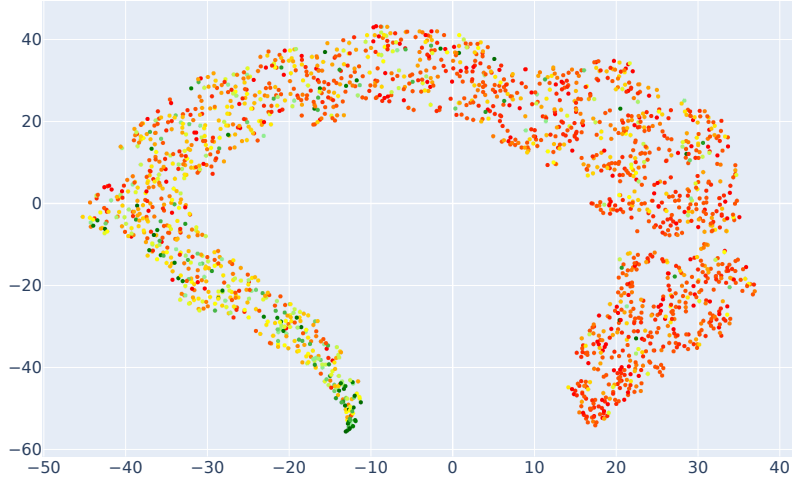


Figure 6: t-SNE visualization of the test queries embedded in the latent space of the fine-tuned BERT on the retrieval task. The ground-truth P@10 performance is encoded via a color map from green to red. The visualization confirms that the fine-tuned BERT predictor learns a meaningful representation of the queries. Best viewed in color.

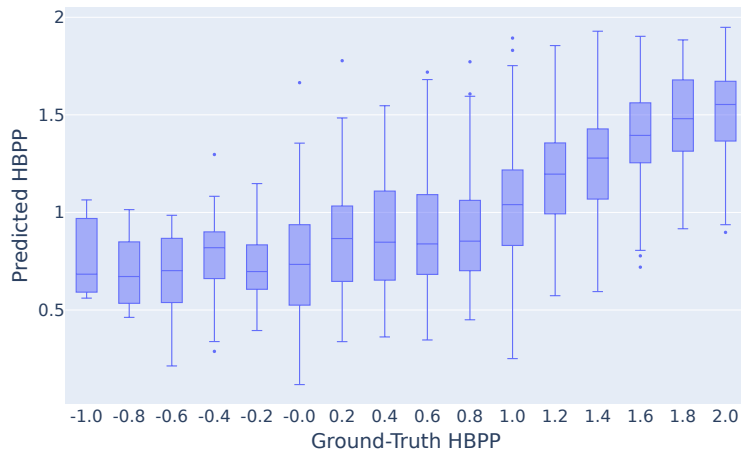


Figure 7: Predicted (vertical axis) vs. reference (horizontal axis) performance for the fine-tuned CLIP predictor, in the text-to-image *generation* setting.

We showcase examples of easy and difficult prompts/queries for the generation and retrieval tasks in Figure 9. The generative models exhibit a clear proficiency with prompts referring to inanimate objects, generating images with high relevance. However, their capability falls short when faced with more intricate prompts involving complex actions based on human-object interactions, leading to inaccuracies in object composition. Such cases exhibit artifacts, such as duplicate or missing body parts and misplaced objects, showcasing the lack of deep understanding in both generative models. The retrieval systems are capable of fetching images for prompts centered around single, loosely-defined objects. However, they struggle when the prompts require images containing multiple, specific elements, retrieving results that only partially match the query. This limitation highlights a gap in the ability of retrieval systems to interpret and respond to the multifaceted nature of some queries. This exploration into both generative and retrieval tasks underscores the nuanced challenges faced by systems in accurately capturing and responding to the inherent complexity of certain prompts. It also reinforces the importance of the prompt/query performance prediction task, setting realistic expectations for the outcomes of both generative and retrieval models, based on the detailed content and structure of the prompts/queries.

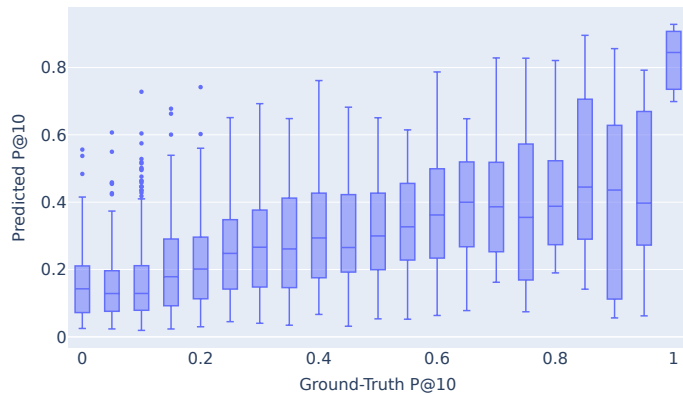


Figure 8: Predicted (vertical axis) vs. reference (horizontal axis) performance for the BERT predictor, in the text-to-image *retrieval* setting.

A.9 Computational Resources

We have employed two types of machines to perform our experiments:

- **Local Hardware:**
 - **GPU:** NVIDIA RTX 3090 with 24GB VRAM
 - **CPU:** Intel i9-10920X @ 3.50GHz
 - **Memory:** 64GB RAM
 - **Storage:** 1TB SSD, 5TB HDD
- **Cloud VM:**
 - **GPU:** NVIDIA A100 with 40GB VRAM
 - **CPU:** 12 vCPUs
 - **Memory:** 85GB RAM
 - **Storage:** 100GB HDD

Our annotation platform was hosted using Google Cloud Provider, with authentication developed using Google Firebase Authentication, and image hosting facilitated by Google Cloud Storage.

By detailing the compute resources utilized, we aim to provide transparency and reproducibility for our research.

A.10 Computational Time Estimation

We present the following estimation of the compute time (in hours) required to fully replicate the experiments detailed in this paper:

- **Pre-processing of the MS COCO dataset:** The extraction of Sentence-BERT embeddings and the subsequent application of the k-means clustering algorithm across the entire corpus of MS COCO captions requires approximately 48 hours.
- **Generative processes:** The generative processes employing both the SDXL and GLIDE methods demand a total time of approximately 120 hours.
- **Preliminary relevance judgments:** The creation of initial relevance judgments for the retrieval task takes 72 hours.
- **Model fine-tuning:** The cumulative time spent on fine-tuning all predictors involved in our study amounts to 48 compute hours.

These estimates are based on the computational resources and configurations described in Section A.9.

	Generative		Retrieval		
Prompts	A woman in white sports gear hitting a tennis ball	This is a yellow and blue double decker bus	Pillows on a bench with a side table and decorative mirrors	A tennis player serves the ball on a clay court	
Stable Diffusion XL					BLIP-2
					
GLIDE					CLIP
					
HBPP	Predicted: 0.421 Ground-truth: 0.250	Predicted: 1.717 Ground-truth: 2.000	Predicted: 0.000 Ground-truth: 0.100	Predicted: 0.934 Ground-truth: 1.000	P@10

Figure 9: Examples of generative (first two columns) and retrieval (last two columns) results for difficult (first and third columns) and easy (second and fourth columns) queries. For the retrieval systems, we show only the top two results. The prompt/query performance values, namely HBPP and P@10, are predicted by the correlation-based CNN. Best viewed in color.